Prediction and Measurement of Surface Mounted Permanent Magnet Motor Performance with Soft Magnetic Composite and Laminated Steel Stator Cores

Munaf Salim Najim Al-Din
Department of Electrical and Computer Engineering
College of Engineering and Architecture
University of Nizwa
P.O. 33 Postal Code 616, Sultanate of Oman
E-mail : munaf@unizwa.edu.om

Abstract: - One of the crucial problems associated with high speed electrical machines is the excessive losses, which give rise to the temperature and thus preventing the machine to run at higher speed. In this paper two different stator cores were used with a surface mounted permanent magnet synchronous motor. The first stator core was made from standard laminated steel and the second is made from soft magnetic composite (SMC) material which is formed by surface-insulated iron powder particles. Experimental and computational assessments to the two prototypes were carried out in this paper.

Key-Words: - Permanent Magnet Motor, Composite and Laminated Steel Stator Cores

1 Introduction

Aerospace, defense and many industrial applications such as centrifugal compressor drives and machine tools require the utilization of high-speed electrical motors. Newly emerged technological advancements in the field of power electronics, digital controls, magnetic materials and high-energy rare-earth permanent magnet materials have led to the utilization of permanent magnet motor drives in such applications [1, 2]. Permanent magnet motors when compared to other types of motors offers the advantages of high power efficiency and compact size. In high-speed applications the major advantages of high speed PM motors is smaller size under a given power, smaller moment of inertia and faster response, and direct connection with other high speed mechanical devices without gears.

The design of high speed permanent machines is not an easy task since several design considerations have to be compromised from the point of view of mechanical and electromagnetic designs. The high speed machines require a rotor construction with good mechanical strength to with stand the centrifugal stresses exerted due to the high speed operations. To overcome this problem magnetic can that encloses the rotor was suggested to provide the required mechanical strength [15]. In the view of electromagnetic design it is important to eliminate losses especially eddy current loss in the stator core of permanent magnet machines. Magnetic losses are responsible for the temperature rise at high speed operations since it is proportional to the square of the frequency, this in turn limits the maximum speed that can be reached due to the dependence of the magnet characteristics on the temperature. It is well know that eddy current loss is proportional to the square of the length of the conducting path provided for the eddy currents. Therefore machines are built from thin ferromagnetic laminations. However this cannot completely eliminate eddy current loss but they are considerably reduced when compared to those of solid ferromagnetic cores.

During the last decade continuing advances in materials research has put in reality the ability to produce high quality material with soft magnetic properties, thus competing with steel laminations at a similar production cost, or even cheaper. When the soft magnetic composite (SMC) materials have appeared on the market, the new perspectives in the electric motor design have been opened.

Recently many research teams started to explore the possibilities of SMC materials in PM machines [4-8]. SMC materials are basically soft magnetic particles such as iron powder connected to each other with an electrically insulated layer [3]. This technology has many advantages to classical laminated core solutions i.e. reduced size and weight, fewer parts and lower manufacturing costs. Therefore, these materials are well suited for use in alternating magnetic fields as the eddy currents are

significantly restricted. This fact allows one to use soft magnetic composite materials in building cores of AC electrical motors; the output is more compact design of electrical machines.

It is the aim of this paper to use SMC material that is made from iron powder to give the desired magnetic properties in an epoxy resin base to rule out eddy current loss. The iron grains may be small enough to make eddy power loss completely negligible as far as minimizing eddy current loss is concerned, the material would be of greater benefit for the stator cores constructions. A prototype of a surface mounted PM machine configuration with conventional laminated steel and SMC stator cores is used. The time-stepping finite elements analysis is used to predict the machine performance, these results are then compared with those obtained experimentally.

2 Motor Prototype

Fig. 1 shows the 2D cross-sectional view of a four poles surface mounted PM motor used in this investigation. The machine parameters are listed in Table 1. The surface mounted magnet blocks are glued onto the rotor. The high energy permanent magnet material NdFeB is used because it offers a high energy density ($BH_{max} \approx 300$ kJ/m^3) and high remanence flux density. Furthermore, motors operated with higher temperatures are no longer a drawback as the new generation of NdFeB magnets retains its magnetic properties up to high temperatures. The considered motor has a stator with 24 slots with symmetrical windings wound in integral slot winding arrangement with number of coils by pole and phase equals 2. Two identical stators were fitted with the surface mounted rotor. The first is a standard laminated core and the second is constructed from SMC material. Replacing the laminated steel sheets by an SMC, i.e. keeping the equal geometry, will enable us to perform accurate analysis for the machine. Table 1, provides the rating of the standard laminated stator, and Fig. 2 shows the B-H curves of the laminated and SMC materials used in this investigation.

The second stator core material has been prepared from iron powder bonded by epoxy which is mixed with suitable hardening material. Since the SMC material is magnetically isotropic the majority of investigators, exploring the use of this new material to date, have focused on utilizing it in applications where the lines of magnetic flux have, or it is useful to add, a significant non-planar component. The permeability of SMC is less than that of the permeability of electrical sheets, used for construction of laminated magnetic cores. But their important advantages are isotropic magnetic characteristics, and the possibility to make shapes more complex than with laminated steel. Another important advantage of SMC could be found in the lower price of small machines, due to the introduction of new more economical manufacturing methods.

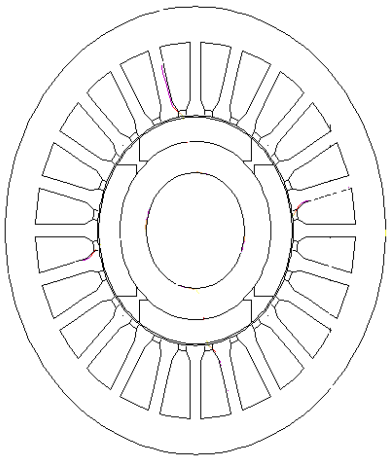

Fig. 1: A cross sectional view of a surface-mounted PMSM

Table 1: Machine Parameters

Phase Voltage (rms)	180 Volts
Phase Current (rms)	3.2 Amp
Rated Torque	0.72 N.m.
Stator Inductance	25 mH
Stator Resistance	5 Ohm
Magnet Flux Linkage	0.0225 Wb
Base Speed	15000 r/min
Number of Poles	4
Number of Slots	24

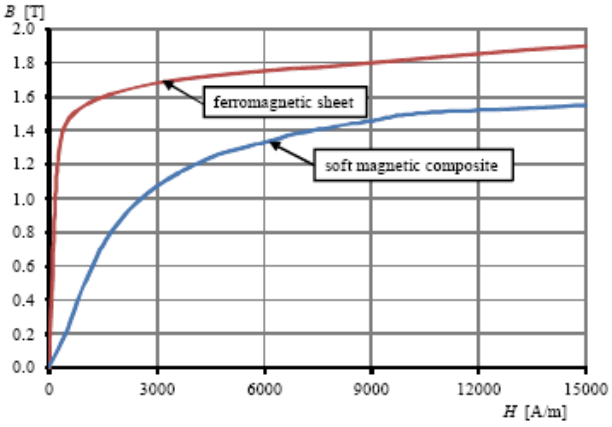

Fig. 2: B-H curve for ferromagnetic and soft magnetic composite sheet

3 Finite Elements Modeling

Computer calculations of the motor performance were performed using 2D time-stepping FEA. In this case, the model was divided and only one pole pitch was analyzed as shown in Fig. 3. The use of time-stepping FEA would assess the validity of the practical results that will be presented in the next section. The effect of magnetic saturation of core fully accounted by the nonlinear BH curves in the FE model.

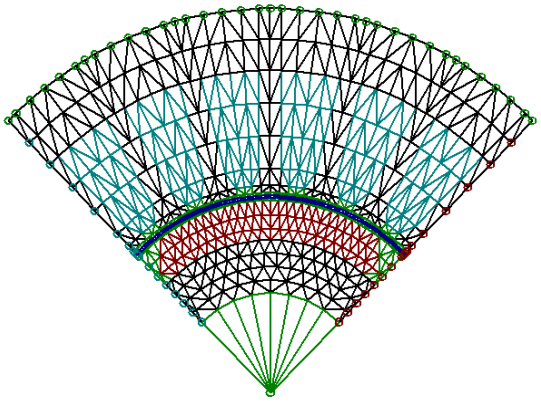

Fig. 3: The FEM model of the machine after formation of mesh

Maxwell equations and the time stepping FEM are used to formulate the magnetic field behavior of the generator. The formulation uses the magnetic vector potential as a variable and the Galerkin method to obtain the set of equations that will be solved numerically. When applying Maxwell's equations a diffusion equation of the following form will be obtained [9-10]:

$$\nabla \times \left(\nu \nabla \times \mathrm{A}\right) = \sigma \frac{\partial \mathrm{A}}{\partial \mathrm{t}} - \mathrm{J}_z + \nabla \times M_o \qquad (1)$$

Where; A is the axial component of the magnetic vector potential, ν is the reluctivity of the material; σ is the conductivity of the material, J_z applied current density and M_0 the magnetization vector . The $\sigma \frac{A}{\partial t}$ represents the induced eddy currents.

The time-stepping FEM method solves generator steady-state and transient performance with each time-step corresponding to a constant mechanical angle of rotor movement. The sliding surface method is used to model the air gap elements [11]. In the model equations, the velocity ω_e is regarded as constant within the sampling time step T_s, assuming that the electrical system's time constant is much smaller than the mechanical time constant. The motor inductances are assumed to be independent of currents. The time derivative can be expressed as:

$$\frac{\partial \mathrm{A}}{\partial \mathrm{t}} = \frac{A(t+\Delta t) - A(t)}{\Delta t} \qquad (2)$$

where Δt is the time step taken between two successive time steps (two successive rotor's relative positions). Equation (1) can now be rewritten as:

$$\nabla \times \left(\nu \nabla \times \mathrm{A}(\mathrm{t}+\Delta \mathrm{t})\right) = \sigma \frac{\partial \mathrm{A}(\mathrm{t}+\Delta \mathrm{t})}{\Delta \mathrm{t}} - \sigma \frac{\partial \mathrm{A}(\mathrm{t})}{\Delta \mathrm{t}} - \mathrm{J}_z(\mathrm{t}+\Delta \mathrm{t}) + \nabla \times M_o(\mathrm{t}+\Delta \mathrm{t}) \qquad (3)$$

As been stated, the FEA is used to assist the validity of the practical results. Therefore, number of motor performance parameters need to be predicted accurately. The following section presents the calculation of the most important parameters that used to determine the performance of the motor. Fig. 4 shows some flux lines plots for the machine.

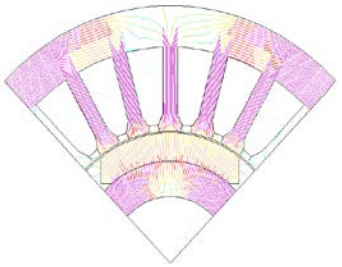

(a)

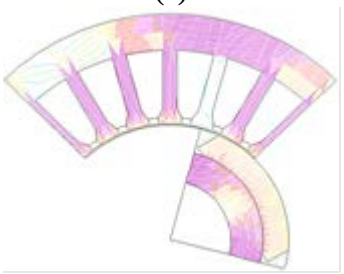

(b)

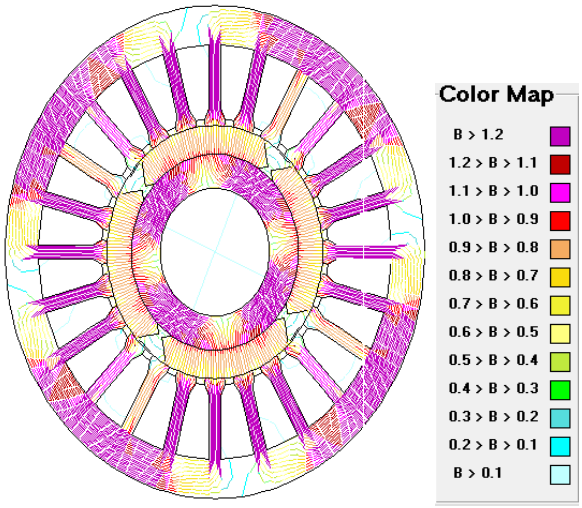

(c)

Fig. 4: The flux plots of the prototype surface-mounted PMSM (a & b) one pole at different time steps (c) complete machine.

3.1 Induced Voltage Prediction

The EMF induced in a machine is calculated from the Faradays's law as:

$$E = -\omega \frac{d\phi}{dt} \quad (5)$$

Where ϕ is the flux linkage over the effective tooth area, ω is the speed and θ is the rotor position in electrical degree. The flux ϕ is related to flux-density as,

$$\phi = \int_s B ds \quad (6)$$

Hence

$$E = -\omega \frac{d}{dt}\left(\int_s B ds\right) = -\omega \int_s \frac{\delta B}{\delta t} \quad (7)$$

On the other hand, from Stoke's theorem

$$E = \oint_l E_i dl = \int_s (\nabla \times E_i) ds \quad (8)$$

where, E_i is the induced electric field intensity. From the equations (7) and (8),

$$\nabla \times E_i = -\frac{\delta B}{\delta t} \quad (9)$$

The flux-density *B* in (9) can be expressed in terms of magnetic vector potential *A*.

Therefore,

$$\nabla \times E_i = -\nabla \times \frac{\delta A}{\delta t} \quad (10)$$

$$\nabla \times \left(E_i + \frac{\delta A}{\delta t}\right) = 0 \quad (11)$$

Since ***curl*** of gradient is zero, the induced electric field intensity per unit length for one turn becomes,

$$E_i = -\frac{\delta A}{\delta t} \quad (12)$$

Integrating E_i over one stator teeth area, multiplying by number of turns and actual length of the machine, gives the induced EMF per phase as,

$$E = -\frac{lN_{ph}}{S} \int_s \frac{\delta A}{\delta t} ds \quad (13)$$

Here, *A* is determined from the time-stepping finite element method.

3.2 Electromagnetic Torque Prediction

The Maxwell's stresses method is used to compute the electromagnetic torque. This method is the general computational method for the evaluation of electromagnetic force exerted at any surface that encloses the rotor, such as the air gap. This force is due to two principal stresses, the first type of these stresses is a tensile stress which acts along the flux lines, while the nature of the second type is compressive and acts at a normal direction to the flux lines. Normally in practical applications, it is more convenient to express these principle stresses in terms of the normal and tangential stress components. The tangential component is the only one of interest in the case of rotating electrical machines, since it is responsible for developing the electromagnetic force in the direction of rotation. While the normal component does not contribute to the torque development because of its resultant around the complete of the rotor cancels due to the symmetry. Periphery Electromagnetic force due to the tangential stress component is given by [12]:

$$F_t = \frac{1}{\mu_o} \oint B_n B_t ds \quad (14)$$

Where (s) is the surface of integration which is taken to be cylindrical, radius (r) is taken at the midway between the rotor and the stator elements to enclose the rotor. In two dimensional treatments, the surface integral in equation (14) reduces to a line integral, and the equation then can be rewritten as:

$$F_t = \frac{rL}{\mu_o} \int_0^{2\pi} B_n B_t d\theta \quad (15)$$

Where ds is substituted by rLdθ, L is the effective axial length of the machine. The electromagnetic torque developed at this surface is:

$$T = \frac{r^2 L^{2\pi}}{\mu_o} \int_0^{2\pi} B_n B_t \, d\theta \quad (16)$$

Direct implementation of equation (16) with finite elements method is very simple and it is not time consuming when the row of elements that represent the mid gap layer are labeled with special material code. The total electromagnetic torque over the path of integration can be found by summing the elemental torque contribution as follows:

$$T = \frac{2\pi r^2 L}{\mu_o} \sum_{e=1}^{E} B_{ne} B_{te} \quad (17)$$

Where E is the total number of air gap elements and (B_{ne}) and (B_{te}) are the normal and the tangential components of flux density evaluated at the centroid of each element.

3.3 Inductance Prediction

The synchronous inductance L_s can determined from the field solution at each time step from the additional stored coenergy in the machine due to the magnetic field that resulted from the an¯nature current [13].The finite element analysis is run first in normal non-linear model and then the model is linearized at the operating point for the parameter calculation. This is done by fixing the reluctivities for each element to correspond with the magnetic field distribution at the moment. After fixing the magnetic properties, an incremental current Δ*i* is applied. The resulting change in the vector potential A is calculated from the linear system of equations. In this case, the reluctivity matrix holds the value from the last iteration step of the nonlinear solution. This ensures that the calculated inductance is incremental, thus representing the tangent of the magnetization curve. The incremental flux linkage Δϕ for all phase windings can be determined and hence L_s The electromotive force (e) is determined by subtracting the effect of the current derivative from the total flux

derivative or from the knowledge of the winding arrangement. The total coenergy ΔW can be found by the summation of all the incremental changes of elemental coenergies ΔW_e. This incremental elemental coenergy can be fundamentally givenby the following equation:

$$\Delta W_e = \int_{B_m}^{B_m + B_a} H dB \quad (18)$$

Where B_m is the flux density due to the field excitation and B_a is the flux density due to the armature winding current. After some manipulations on equation (18), the additional coenergy stored in each element can be given by:

$$\Delta W_e = \frac{B}{2\mu} \quad (19)$$

The total change in the coenergy W_m is then can be found by using the following relation:

$$\Delta W_m = \sum_{i=1}^{E} \Delta W_i L \quad (20)$$

Where (E) is the total number of elements and (L) is the axial length of the machine. From Equation (20), the synchronous reactance per phase can be given by the relation:

$$X_s = \frac{4\Delta W_m}{3I^2} \omega L \quad (21)$$

Where ω is the angular speed and I is the peak phase current.

The synchronous reactance that can be obtained from the last equation represents the total reactance including the leakage reactance. Leakage reactance is important to be total determined, and is classified into, slot leakage, Zig-zag leakage, end winding leakage and harmonics leakage. Only the first type can be obtained from the two dimensional treatment from numerical evaluation of the energy stored in the slots.

3.4 Magnetic Losses

The PM motor contains a standstill stator and a moving rotor. In establishing the meshes for the analysis, the rotor is moved and positioned at each time step such that it does not disturb the integrity of the mesh structure as it moves. The initial meshes of the stator and the rotor are generated such that half of the air gap belongs to the stator and the other half to the rotor. A stator mesh and a rotor mesh share the same boundary at the middle of the air gap. The inner stator circumference at the air gap and the outer rotor circumference are divided into equal steps so that their nodes coincide. To provide for movement of the rotor, the time step is chosen so that the angle or length of each step is equal to the interval between two neighboring nodes along the mid air gap. Because of periodicity of the magnetic field, only one pair of poles needs to be modeled. Similarly, because of the half-wave symmetry of flux density, only half of the time period needs to be calculated. The radial and circumferential components of flux density at time step in the volume element are evaluated as [14]:

$$P_e = \frac{p}{2} \sum_{m=1}^{M} A_m l_{fe} \frac{2k_e}{T} 2 \int_0^{T/2} \left(\frac{dB}{dt}\right)^2 dt \quad (22)$$

Where N is the total number of steps in the half time period (T/2), L_{fe} is the stator core length, A_m is the area of element m, and M is the total number of elements in the stator. In a similar manner the hysteresis losses are computes as follows:

$$P_h = 2\pi f k_h l_{fe} \sum_{m=1}^{M} A_m B_m^{\beta} \quad (23)$$

4 Experiment and Computational Assessments

SMC stator has lower relative permeability when compared to that of steel laminations, and this cause the magnetic circuit of the stator to be of higher reluctance than that of the rotor. With this higher reluctance the magnetic field density in the air-gap and in the stator core is lower than that in the laminated steel core, as it can be noticed in Fig. 5. Furthermore, the operating point of the magnet in the powder stators drops down due to the high reluctance of the magnetic circuit. As a consequence of these two effects, the air gap flux density in the case of iron powder stators, and this greatly affect the synchronous performance of the machine in terms of the open circuit induced voltage and the torque production where they can be noticed from Fig 6 and Fig. 7.

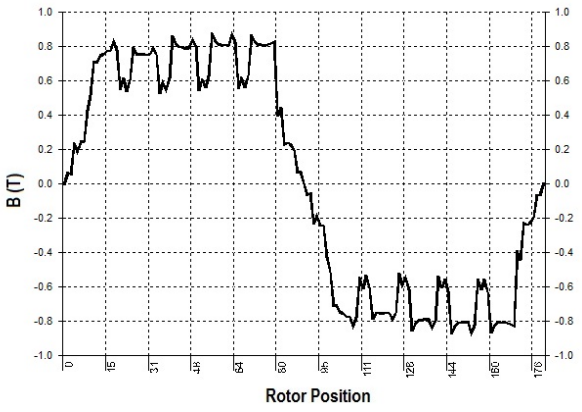

Fig. 5-a: Flux density variation in the air-gap for laminated core machine

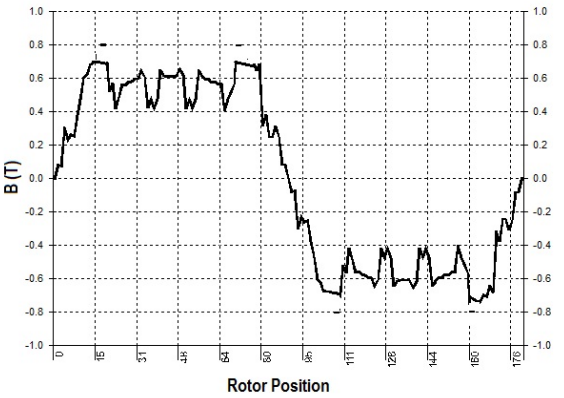

Fig. 5-b: Flux density variation in the air-gap for SMC core machine

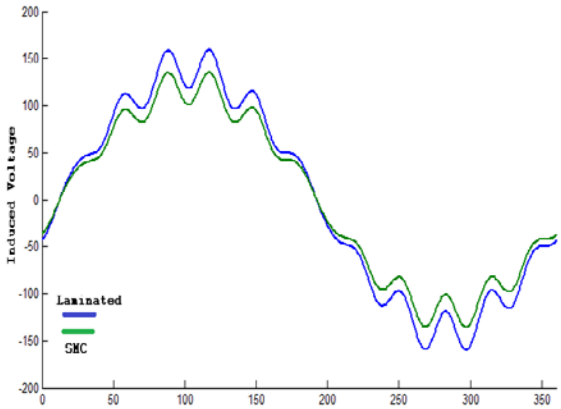

Fig. 6: No-Load induced voltage waveform

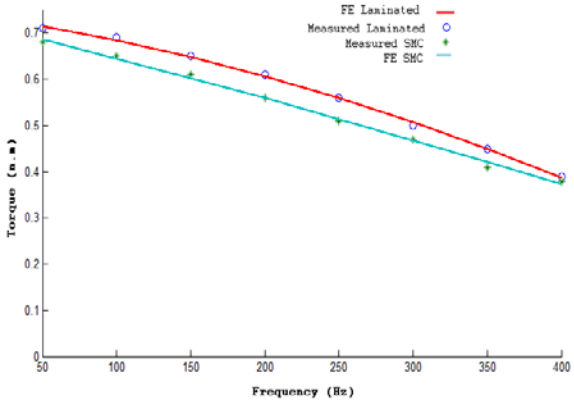

Fig. 7: Maximum torque variation with frequency

Since the motors designed to run at high speed, the losses considerably affect the performance and limit the maximum speed that can be reached. The losses can be classified as being due to three types of mechanisms namely; copper loss of the stator winding, wind age and friction loss and the magnetic losses. The I^2R losses in small machines are quite high, and they increase with frequency with lower percentage than that with magnetic losses, however temperature effects have to be considered in the evaluation of the effective resistance. Mechanical loss is also significant at high speeds and it greatly affects the efficiency of the rotor, magnetic losses are almost proportional to the square of the frequency and they result when there is flux fluctuations within the ferromagnetic materials. Both the stator and the rotor cores are subjected to this flux variation, but the stator is responsible for the most of the magnetic losses in the synchronous machines especially eddy current loss. This loss depends on the peak value of flux density and its distribution, frequency of operation and upon the type of the magnetic materials used. With the SMC machine lower magnetic losses are noticed, and this is not surprising since the materials has high resistance to eddy currents and is subjected to a low magnetic field. Fig. 8 shows the no load magnetic losses variation with the frequency for both machines while Fig. 9 and Fig. 10 show the variation of the efficiency with load at 50Hz and 400 Hz respectively. The maximum torque reduces with the increase of the frequency as shown in Fig. 8. This reduction is mainly attributed to the opposing torque resulting from the increased magnetic losses, and the large windage and friction losses, where both increases with the increase in the frequency of operation.

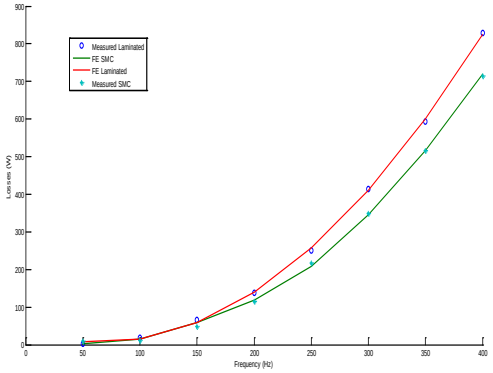

Fig. 8: Variation of no-load magnetic losses

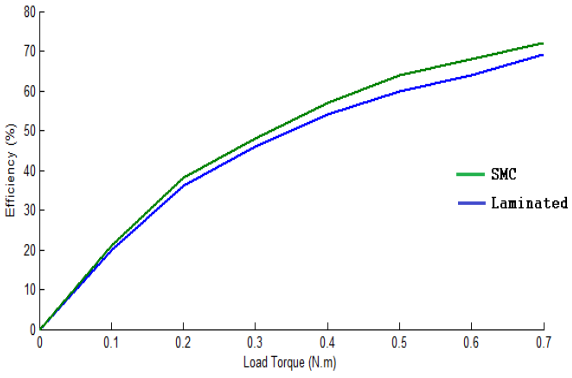

Fig. 9: Variation of the efficiency at 50 Hz.

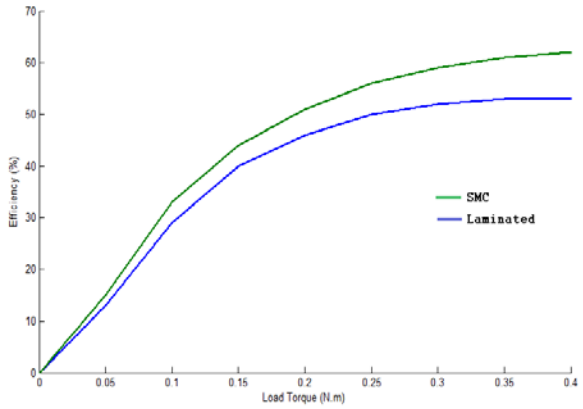

Fig. 10: Variation of the efficiency at 400 Hz.

CONCLUSION

The advantages of application soft magnetic composites in electrical machines have been discussed. The experimental setup for testing the performance of high speed PM motor has been elaborated and described. According to obtained preliminary results it can be noticed that the efficiency of full drive system is rather high. Therefore it can be concluded that SMC technology can be an high efficiency alternative for high speed electrical machines working at frequency above 400 Hz. Nevertheless the final prove will be the comparison of drives with SMC and classical laminated core machines in the same conditions. The work presents a comparison of performance of both motors prototypes - with SMC and classical laminated steel core working in different operation modes.

References

[1] Limei Zhao, Chan Ham, Liping Zheng, Thomas Wu, Kalpathy Sundaram, Jay Kapat and Louis Chow: "A Highly Efficient 200 000 RPM Permanent Magnet Motor System", IEEE Tans. On Mag., Vol. 43, No. 6, June 2007, pp. 2528-2530.

[2] Roy Perrymam: "High Efficiency High Speed PM Motors for the More Electric Aircraft", Proceedings of the 6th WSEAS International Conference on Power Systems, Lisbon, Portugal, September 22-24, 2006, pp. 368-375.

[3] B. Jankowski, C. Jedryczka, D. Kapelski, W. Szelag, B. Slusarek, R. M. Wojciechowski: "High Speed Permanent Magnet Motor with Powder Magnet", International Symposium on Power Electronics, Electrical Drives, Automation and Motion, 2012, pp. 1230-1234.

[4] Yunkai Huang, Qiansheng Hu, Jianfeng Zhao Jianguo Zhu and Youguang Guo: "Comparative Study of High-Speed PM Motors with Laminated Steel and Soft Magnetic Composite Cores",

[5] Youguang Guo, Jianguo Zhu and D. G. Dorrell: "Design and Analysis of a Claw Pole Permanent Magnet Motor with Molded Soft Magnetic Composite Core IEEE Tans. On Mag., Vol. 45, No. 10, Oct., 2009, pp. 4582

[6] Chengdu, China: "Design and Analysis of a Permanent Magnet Motor with SMC Core for Driving Dishwasher Pump Proceedings of 2009 IEEE International Conference on Applied Superconductivity and Electromagnetic Devices, September 25-27, 2009, pp.

[7] Zhuonan Wang, Yuji Enomoto, Motoya Ito, Ryoso Masaki, Shigeki Morinaga, Hiromitsu Itabashi and Shigeho Tanigawa: "Development of a Permanent Magnet Motor Utilizing Amorphous Wound Cores", IEEE Tans. On Mag., Vol. 46, NO. 2, Feb. 2010, pp.570

[8] Kang Geon Il, Han Man Seung, Yang Seung Hak, Lim Young Cheol: "The Study on BLDC Motor Compressor Using SMC",

[9] M. A. Jabbar, , Zhejie Liu, and Jing Dong: Time-Stepping Finite-Element Analysis for the Dynamic Performance of a Permanent Magnet Synchronous Motor, IEEE Transactions on Magnetics, Vol. 39, No. 5, Sept. 2003, pp. 2621-2623.

[10] Joao Pedro A. Bastos and Nelson Sadowski : "Electromagnetic Modelling by Finite Element methods"; Marcel Dekker, Inc. 2003.

[11] W. N. Fu, Zheng Zhang, P. Zhou, D. Lin, S. Stanton and Z. J. Cendes: "Curvilinear finite elements for modeling the sliding surface in rotating electrical machines and its applications"; IEEE International Conference on Electric Machines and Drives IEMDC.2005, 2005, pp. 628-634.

[12] K. Komeza, A. Pelikant, J. Tegopoulos and S. Wiak, Comparative Computation of Forces and Torques of Electromagnetic Devices by Means of Different Formulae, IEEE Trans. on Magnetics, Vol. 30, No. 5, 1994, pp.3475-3478.

[13] Jacek F. Gieras, Ezio Santini, and Mitchell Wing, Calculation of Synchronous Reactances of Small Permanent-Magnet Alternating-Current Motors: Comparison of Analytical Approach and Finite Element Method with Measurements, IEEE Trans. on Magnetics, Vol. 34, No. 5, Sept. 1998, pp.3712-3720.

[14] Roshen, W: "Iron Loss Model for Permanent Magnet Synchronous Motors," IEEE Trans. Magn., Vol. 43, No. 8, 2007, pp. 3428–3434.

[15] Al-Din M.S.N. , Kader, A.F. and Al-Samarai, J.: "A new method to compute eddy current losses by the finite elements method", IEEE Industry Applications Conference, Thirty-Second IAS Annual Meeting, IAS '97, Vol. 1, 1997, pp. 3-9.